

LEWIS RESEARCH CENTER
11-32-PR
190168
198



Electromagnetic Properties of Ice Coated Surfaces

by

A. Dominek, E. Walton, N. Wang and L. Beard

The Ohio State University

ElectroScience Laboratory

Department of Electrical Engineering
Columbus, Ohio 43212

(NASA-CR-184780) ELECTROMAGNETIC PROPERTIES
OF ICE COATED SURFACES Semiannual Report
(Ohio State Univ.) 19 p CSCI 20N

N89-20355

Unclas
G3/32 0190168

Semi-Annual Report No. 720964-2

Grant NAG3-913

February 1989

National Aeronautics and Space Administration

Lewis Research Center

Cleveland, OH 44135

NOTICES

When Government drawings, specifications, or other data are used for any purpose other than in connection with a definitely related Government procurement operation, the United States Government thereby incurs no responsibility nor any obligation whatsoever, and the fact that the Government may have formulated, furnished, or in any way supplied the said drawings, specifications, or other data, is not to be regarded by implication or otherwise as in any manner licensing the holder or any other person or corporation, or conveying any rights or permission to manufacture, use, or sell any patented invention that may in any way be related thereto.

Contents

List of Figures	iv
1 Introduction	1
2 Scattering Mechanisms	2
3 Tunnel Simulation	7
4 Conclusions	13

PRECEDING PAGE BLANK NOT FILMED

List of Figures

2.1	Rough ice simulation with artificial ice on almond test body. Test region is approximately 18" from tip to tip.	4
2.2	Swept frequency measurement and transient signature for rough ice simulation. Solid line - measurement, Dashed line - analytical model calculation.	5
3.1	Ice tunnel simulation for RCS measurements.	8
3.2	Stability test of the simulation tunnel.	10
3.3	Measured response of a corner reflector 10 feet from test horns.	11
3.4	Measured response of a corner reflector 14 feet from test horns.	12

Chapter 1

Introduction

The presence of ice formations on an aerodynamic structure affects not only the aerodynamic performance but also the anticipated radar cross section (RCS) of the structure. Few studies have been performed to investigate the influence of ice on the RCS values for a structure. It is important to understand the mechanisms involved that control the RCS signature. Research to characterize the impact of ice related RCS signatures is presently underway. So far, all of the studies have involved simulations with artificial ice geometries (both experimentally and analytically) as one area of effort. Another area of effort is to provide the measurement capability of monitoring the RCS of a structure in an existing NASA Lewis existing icing tunnel.

Chapter 2

Scattering Mechanisms

The scattering from a structure can many times be modeled in terms of various mechanisms. The scattering mechanisms may not be only due to the ice itself but also to the mechanical structure involved when deicing approaches are also considered. The conventional deicing approach is to flow ethylene glycol over the structure. This approach is not invasive to the aerodynamic contour and hence, does not impose a significant concern from this viewpoint. A more modern deicing approach is to use a pneumatic boot which involves the mechanical stressing of ice to break it off. The stressing force is developed by the expansion of parallel rubber tubes internal to the the aerodynamic contour. Such an approach naturally has a corrugated surface contour due to the discrete internal rubber tubes. The effect of a similar metal surface is discussed in [1]. The major concern from a corrugated surface is the generation of very strong grating lobes if the surface variation has a half wavelength periodicity. Such a surface variation has been modeled for a corrugated ice surface in [2].

The initial RCS measurements made to demonstrate the significance of scattering from a rough ice surface were made with a material (supplied by NASA Lewis) which simulated ice in terms of its bulk electrical properties. Figure 2.1 illustrates the tested geometry. The artificial ice was randomly positioned on a metal plate that was flush mounted into a low cross section

test body. The measured return was solely due to the positioned material since the cross section of the test body was much lower [3]. A typical measured swept frequency RCS response is shown in Figure 2.2. The sample was illuminated from 20° from grazing with the electric field in the plane of incidence. Also shown is a bandlimited impulse signature generated from the measurement which demonstrates the surface scattering of the material. The material particles were generally .25 to .5 inches across and the time domain signature indicates a positional randomness among the particles since there is no evidence of any distinct scattering centers. The RCS levels are in the -20 to -30 dBsm range for a surface area of 47.3 square inches. These values can be scaled based upon area to estimate the return for larger areas when the scattering between scattering centers is random. For example, if the measured return is -20 dBsm for a given area, the return from an area twice that size would be -17 dBsm or 3 dB more.

The measured response was analyzed as being generated from electrically small, random, dielectric hemispheres on a perfectly conducting surface. The dashed line in Figure 2.2 is the result. One hundred scatterers were used in this calculation with diameter size variations from .25 to .5 inches. The scattering from electrically small (characteristic dimension much smaller than a wavelength) objects is essentially geometry independent. The calculation required the constitutive parameters of the material which were obtained with X-band waveguide measurements. The measured constitutive parameter values are $\epsilon_r = (2.9, j0)$ and $\mu_r = (1., j0.)$. Similar measurements for a frozen sample of deionized water resulted in values of $\epsilon_r = (3.25, j0.)$ and $\mu_r = (1., j0.)$.

The scattering from ice so far has concerned itself with electrically small, random ice particles in both size and position. However, physically larger ice formations are geometry dependent and have to be studied on an individual basis. An example of this is when an inch or two of ice may form an

ORIGINAL PAGE IS
OF POOR QUALITY

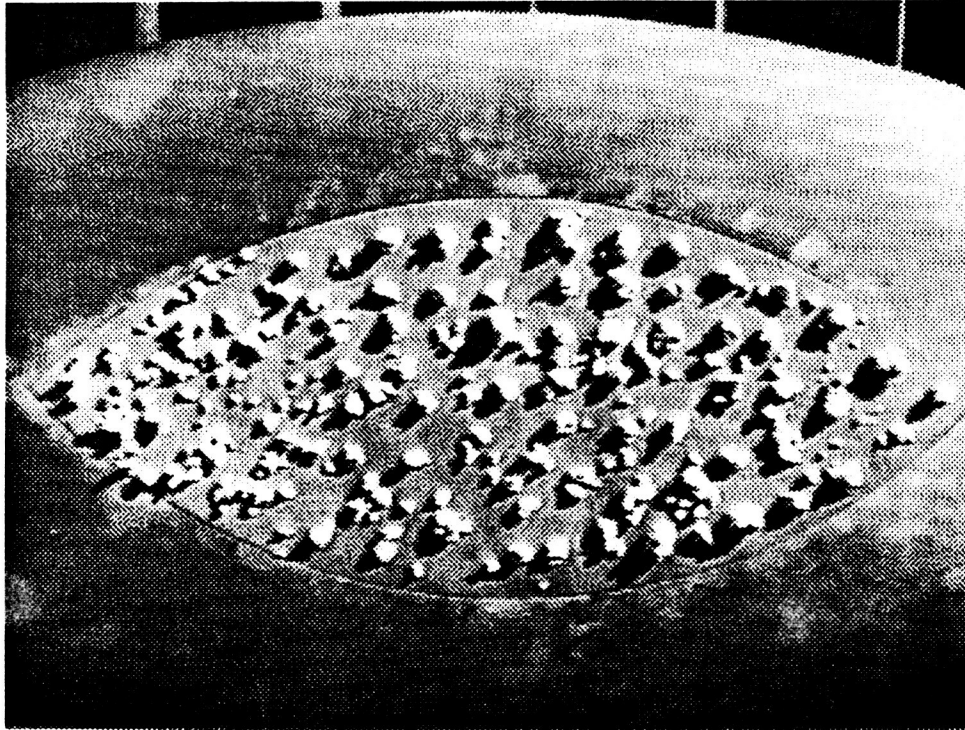


Figure 2.1: Rough ice simulation with artificial ice on almond test body.
Test region is approximately 18" from tip to tip.

ORIGINAL PAGE IS
OF POOR QUALITY

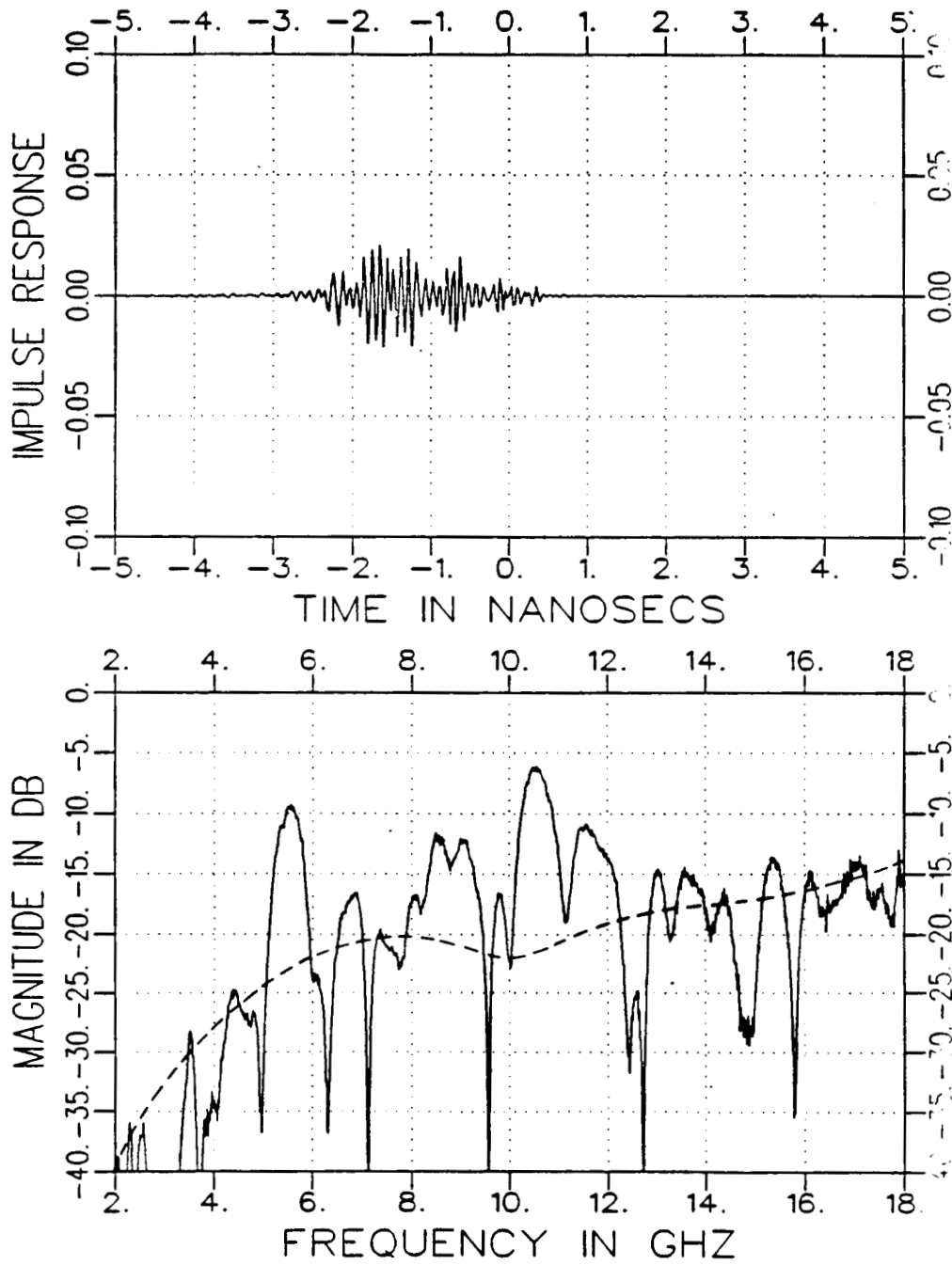


Figure 2.2: Swept frequency measurement and transient signature for rough ice simulation. Solid line - measurement, Dashed line - analytical model calculation.

extension on the rim of a jet inlet. Other scattering mechanisms may exist when all the ice is not successfully removed through a deicing process. For example, the pneumatic boot approach may successfully remove the ice on the surface itself but it will leave some ice to form along the boot. This process will form an edge of ice which acts as an electrical discontinuity in which scattering can occur.

Another potential scattering mechanism involves the presence of surface waves. Ice, especially glaze ice, may guide energy to other areas of the surface to scattering from a discontinuity. Ice itself, when formed from deionized water, is very lossless and can provide a good guide of energy. A similar guide of energy may be the residual ethylene glycol fluid to prevent ice build up. However, if the fluid is not sufficiently lossy, it can readily be made so.

Chapter 3

Tunnel Simulation

A major effort of this research is to develop the capability to perform real time RCS measurements in the NASA Lewis icing tunnel. The benefit gained is the ability to obtain actual RCS values for various realistic ice formations. A system is presently being designed and tested using a HP 8510 network analyzer as the core piece of instrumentation with accompanying software for data collection and signal processing. A 24 foot long tunnel with metal walls was erected at OSU to aid in this development to simulate the actual electromagnetic conditions that would exist in the icing tunnel. The internal cross section of the test tunnel is 9 feet wide and 6 feet high. Figure 3.1 is a photograph an interior portion of this tunnel with a styrofoam mount used to support the test scatters.

The ability to accurately acquire RCS measurements is dependent upon two factors. The first factor is the electrical stability of the radar and test tunnel. The measurement procedure generally requires a vector subtraction of data measured when the ice is present and absent on the structure. This eliminates most returns that are ice independent. This procedure will not work if the subtraction of two like measurements does not result in a low level. The other factor is to be able to distinguish between desired and undesired terms which are left after the subtraction process. This aspect is very important since multiple images of the structure which supports the

ORIGINAL PAGE IS
OF POOR QUALITY

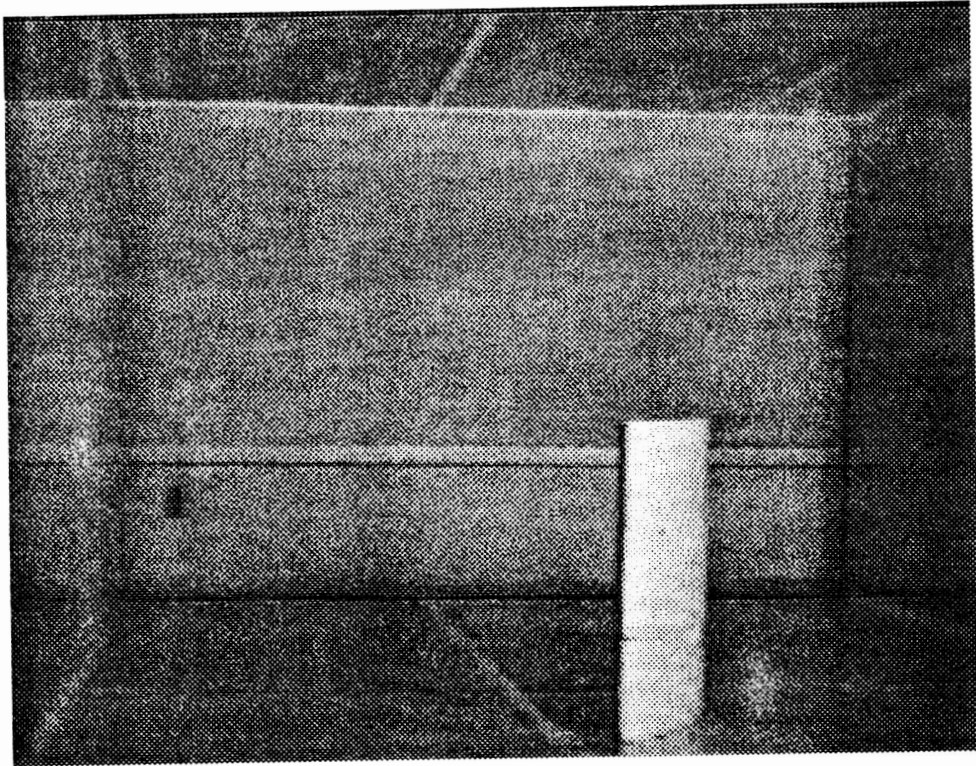


Figure 3.1: Ice tunnel simulation for RCS measurements.

ice formation can readily exist. The elimination of these undesirable returns can be accomplished in a variety of signal processing techniques. The most basic technique is the time domain (down range) gating of desired terms from the total signature from a swept frequency measurement [4]. Another technique is through modified (near field) synthetic aperture radar (SAR) techniques [5,6] for cross range gating. These SAR techniques require a significant amount of measured data.

The initial evaluation of the system was performed using the HP 8510 network analyzer configured in a two horn transmit-receive mode with the horns positioned 3 feet above the floor of the tunnel and centered between the side walls. Swept frequency measurements were taken between 2 and 10 GHz. Figure 3.2 illustrates the stability of this system when two similar measurements are subtracted which were generated 7 hours apart. This result is calibrated by scaling it with the measured and known responses of a 9" trihedral corner reflector.

Figures 3.3 and 3.4 illustrate the measured response of a 9 inch trihedral corner reflector positioned 10 and 14 feet from the horns. These responses were generated by subtracting measurements which had the reflector present and absent from the tunnel. Note the variation of the desired signal level as a function of range and the other smaller returns delayed in time from the main return of the corner reflector. These other terms may be due to multiple reflections from the metal walls of the test chamber.

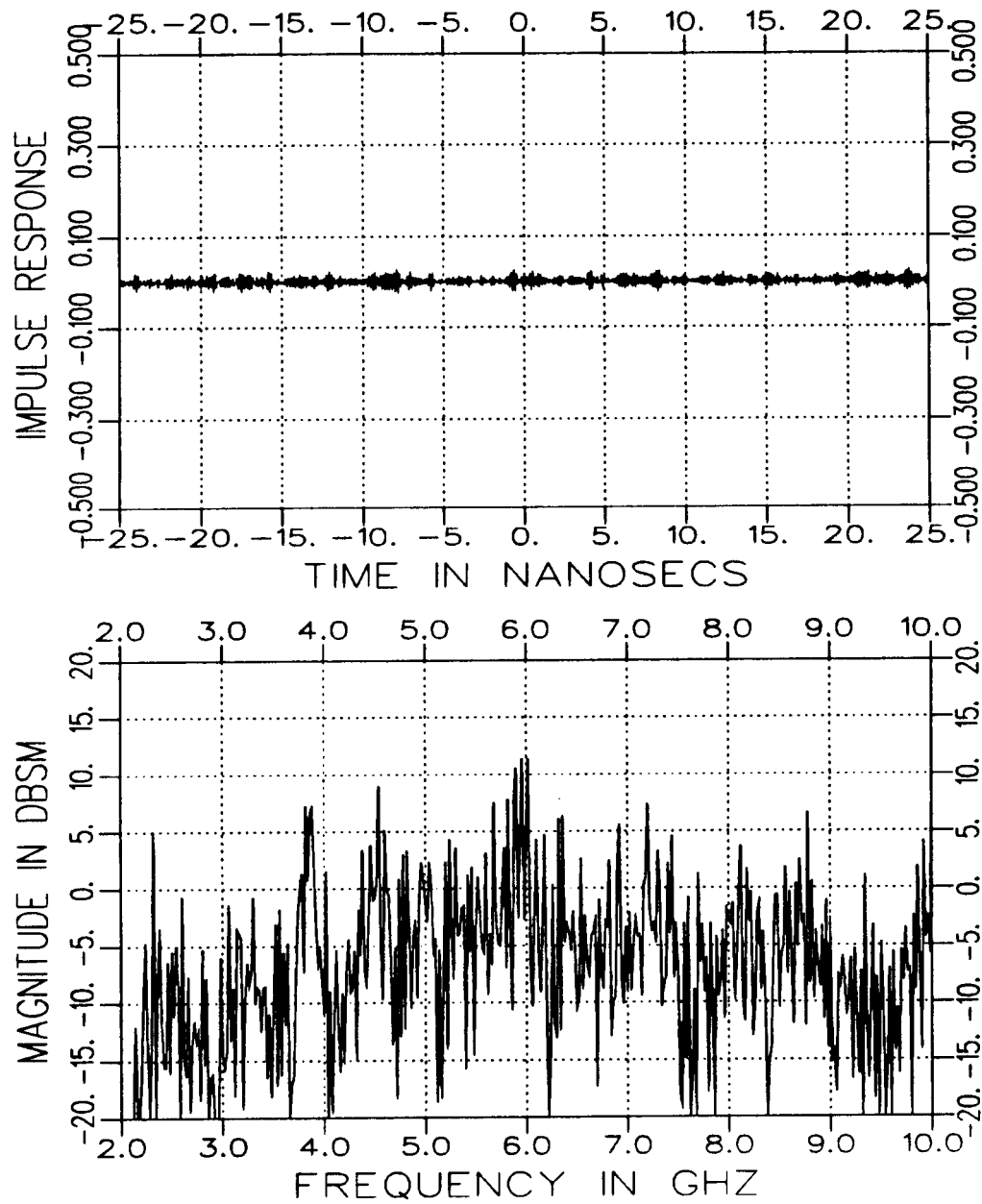


Figure 3.2: Stability test of the simulation tunnel.

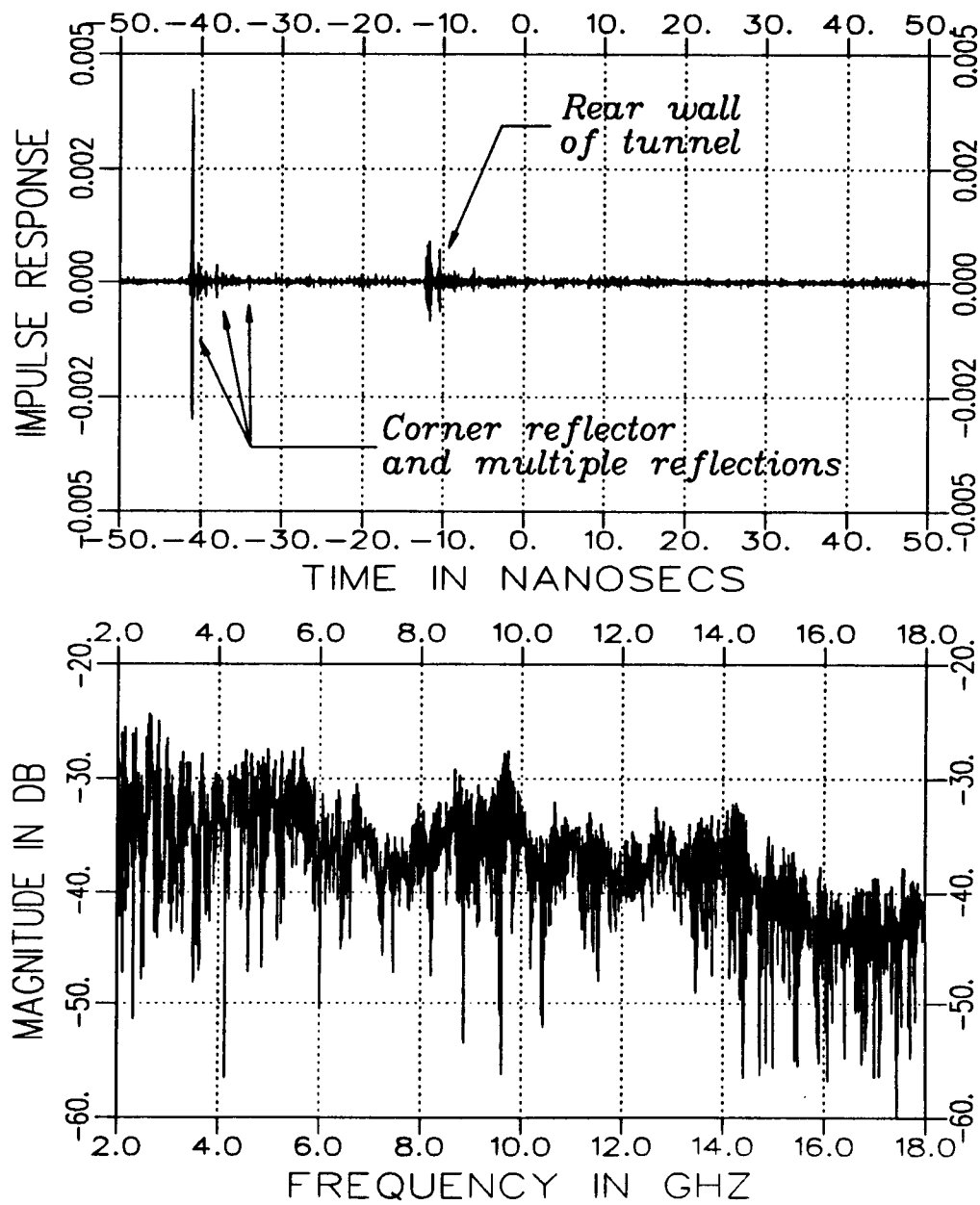


Figure 3.3: Measured response of a corner reflector 10 feet from test horns.

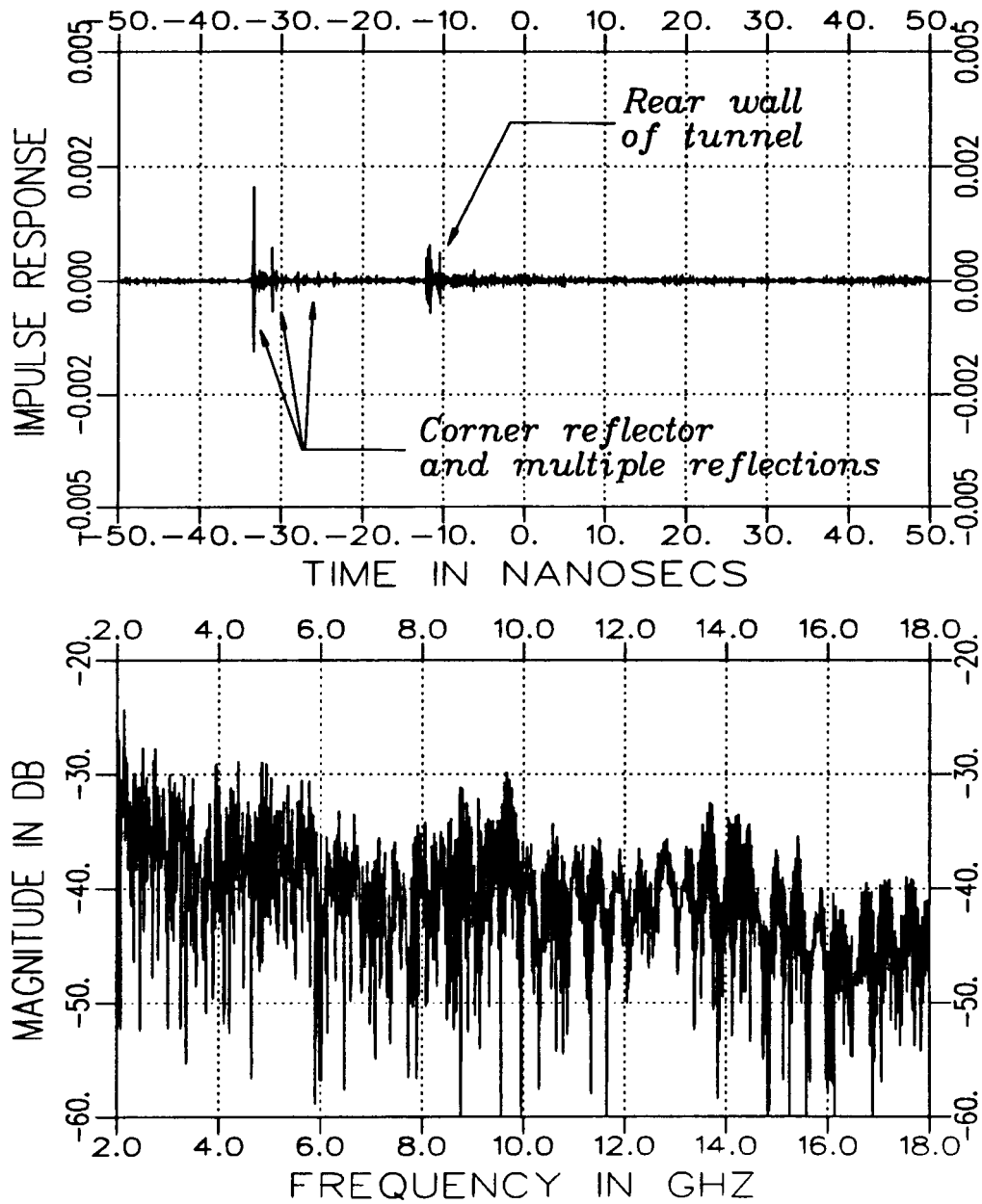


Figure 3.4: Measured response of a corner reflector 14 feet from test horns.

Chapter 4

Conclusions

Future work for analytical modeling will be centered around calculating the response from shaped ice structures that are naturally formed (those that are not electrically small) and thus formed from the residual ice left on the aerodynamic surface after a pneumatic deicing approach has been applied.

The major work for the tunnel simulation is to improve the noise level of the system to measure the low signal levels which are present. The approaches available involve either hardware modification or software implementation. The hardware modification incorporates the use of a modulated radar configuration (pulsed-cw) to achieve the necessary improvement. The software approach uses signal processing of a modified SAR imaging concept which requires multiple measurements.

Bibliography

- [1] A.K. Dominek, H.T. Shamansky and R.M. Wood, "Backscatter from a Periodic Rough Surface at a Near Grazing Incidence," Report 716148-24, The Ohio State University ElectroScience Laboratory; Prepared under Grant NSG 1613, NASA Langley Research Center, October 1987.
- [2] K.M. Lambert and L. Peters, Jr., "Calculation of the effects of ice on the backscatter of a ground plane," Report No. 720964-1, The Ohio State University ElectroScience Laboratory, prepared under Grant NAG3-913 for NASA Lewis Research Center, September, 1988.
- [3] A.K. Dominek, H.T. Shamansky, R.M. Wood and R. Barger, "A Low Cross Section Test Body," Conference Paper, Antenna Measurements Techniques Association, Seattle WA, Sept. 1986.
- [4] A.K. Dominek, L. Peters, Jr. and W.D. Burnside, "A Time Domain Technique for Mechanism Extraction," IEEE Trans. on Antennas and Propagation, Vol. AP-35, No. 3, pp. 305-312, March 1987.
- [5] D.R. Koberstein, "Near Field Synthetic Aperture Imaging of Probe Data for Scattering Studies of the ElectroScience Laboratory Compact Range," Report 718331-7, The Ohio State University ElectroScience Laboratory; Prepared under Contract GR9300, Boeing Aerospace Company, September 1986.
- [6] D.L. Mensa, *High Resolution Radar Imaging*, Dedham, MA, Artech House, 1981, pp. 103-118.

REPORT DOCUMENTATION PAGE	1. REPORT NO.	2.	3. Recipient's Accession No.
4. Title and Subtitle ELECTROMAGNETIC PROPERTIES OF ICE COATED SURFACES		5. Report Date February 1989	
7. Author(s) A. Dominek, E. Walton, N. Wang and L. Beard		6.	
9. Performing Organisation Name and Address The Ohio State University ElectroScience Laboratory 1320 Kinnear Road Columbus, OH 43212		8. Performing Org. Rept. No. 720964-2	
12. Sponsoring Organisation Name and Address National Aeronautics and Space Administration Lewis Research Center Cleveland, OH 44135		10. Project/Task/Work Unit No.	
15. Supplementary Notes		11. Contract(C) or Grant(G) No. (C) (G) N 8 G3-913	
16. Abstract (Limit: 200 words) The electromagnetic scattering from ice coated structures is examined. The influence of ice is shown from a measurement standpoint and related to a simple analytical model. A hardware system for the realistic measurement of ice coated structures is also being developed to use in an existing NASA Lewis icing tunnel. Presently, initial measurements have been performed with a simulated tunnel to aid in the development.		13. Report Type/Period Covered Semi-Annual	
17. Document Analysis a. Descriptors		14.	
b. Identifiers/Open-Ended Terms			
c. COSATI Field/Group			
18. Availability Statement	19. Security Class (This Report) Unclassified	21. No. of Pages 14	
	20. Security Class (This Page) Unclassified	22. Price	